IR Absorption Tomography for Active Combustion Control
Final Report on ONR Grant N00014-99-1-0447

F. C. Gouldin

College of Engineering, Cornell University

Ithaca, N Y 14853

Summary: The goals of our research were to further the development of IR absorption tomography as a sensor for closed-loop control of combustion and propulsion systems of interest to the Navy, to apply IR absorption tomography to study mixing in forced-jet actuators, and to use POD analysis to investigate large scale structures in reacting jet flows and the potential for reduced order models of jet actuators. In the last year of the grant we expanded its scope to include the development of a camera system for measuring chemiluminescence from combustors to obtain a semi-quantitative measure of combustion heat release dynamics. Our research has been in collaboration with Drs. Grinstein and Kailasanth of the NRL and recently with Dr. Robert Schefer of Sandia National Laboratories. Major accomplishments during the grant were completion of an IR absorption facility and measurements on forced, square jets, refinement of our tomographic reconstruction algorithm – Adaptive Finite Domain Direct Inversion (AFDDI) - analysis of large eddy simulations of forced, reacting rectangular jets using proper orthogonal decomposition (POD), and in the past year work on the development of a new camera system for chemiluminescence emission tomography to obtain spatially resolved data on heat release dynamics. This work was a significant portion of two PhD theses, was reported in four AIAA preprints and is the subject of two papers in preparation for publication and an article appearing in a book based on papers presented at the 15th ONR Propulsion Meeting.

20030806 118

Contents

Introduction

Our overall goal was to develop and apply multiple line-of-sight (LOS) infrared (IR) absorption and emission tomography for problems of combustion control in naval propulsion systems such as ramjets and turbojets. For IR absorption tomography, the attenuation of radiation along multiple LOSs in a common plane is measured, and the data are used to reconstruct the spatial distribution, in the measurement plane, of the radiation-absorbing chemical species, e.g., CO_2, CO and NO. For emission tomography the intensities of chemiluminescence emissions along multiple LOSs are measured and used to reconstruct spatial distributions of mean emission intensity and elements of the power spectral density of these emissions. In addition during the grant period, we collaborated with Drs. Grinstein and Kailasanath in the study of forced jet actuators and the use of proper orthogonal decomposition (POD) as a tool to characterize large scale structures in these flows and to evaluate the potential of reduced order modeling.

Many aspects of combustor performance such as efficiency, signature and pollutant emissions depend in whole or part on mixing processes. These processes, in turn, depend on the flow configuration, large scale flow structures - macro-mixing - and on molecular transport - micro-mixing. Tomography provides data on the state of macro-mixing. Chemiluminescence emissions, especially from OH* and CH* are proportional to the local heat release rate, and consequently emission data are valuable for studying variations in heat release rate. For example, measurements on unsteady flames would provide data for comparison to large eddy simulations (LES) of combustion instability.

For practical reasons the number of LOS measurements is finite, and the tomographic reconstruction problem is ill posed. We have developed two reconstruction methods for cases where optical access is restricted, and the number of measurement LOSs is limited. One method, adaptive Finite Domain Direct Inversion (AFDDI), requires 100 or more LOSs [1,2,3], while the other, Tomographic Reconstruction via a Karhunen-Loéve Basis (TRKB), requires far fewer [4,5]. Because it requires very few LOSs, we believe that this latter method has potential for use in sensing for feedback control of combustion systems where optical access is limited. TRKB requires considerable *a priori* information in the form of a set of expected distributions, the training set. This set is analyzed via POD to yield a set of basis functions, the Karhunen-Loeve (K-L) eigenfunctions that are used for reconstruction. These training sets could come from measurements on prototype equipment or from computational combustion simulations.

The K-L eigenfunctions are empirical eigenfunctions and form an optimal basis set for representing the distributions of the set of distributions from which they are derived. This means that a subset of the K-L eigenfunctions can always be found that, on average, is equally good or better than any other set of the same size for representing the distributions in the original set. We have used this property to evaluate the potential for reduced order modeling of the reacting rectangular jet simulations of Grinstein and Kailasanath [8, 9].

In the last year of the grant, we began work on a compact camera system – both hardware and software - for chemiluminescence emission tomography measurements of heat release dynamics in combustion systems. The camera is a single lens reflex camera with a linear array detector mounted in the focal plane. The camera is compact, portable and easy to align. With it simultaneous emission measurements along 32 LOSs can be made. In addition, we have discussed with Pratt & Whitney a project to design the optical configuration for an IR laser based

tomographic temperature pattern factor sensor. Contract negotiations with Pratt and Whitney for our work are underway.

Absorption and Emission Tomography

In absorption tomography, laser beam transmission measurements are made along many LOSs distributed over several viewing angles, θ. For our measurements, LOSs sharing a common viewing angle are parallel to each other and defined by their offset s, Figure 1. For isothermal conditions, line integrals of number density, $n(x,y)$, over a LOS can be related to the laser beam transmission, Eq. (1).

$$p(s,\theta) = -\ln \frac{I_\nu^t}{I_\nu^0} = \sigma \int_{-T}^{T} n(x,y)dt \qquad (1)$$

The projection $p(s,\theta)$ is the line integral of $n(x,y)$ along the LOS defined by s and θ times the absorption cross section σ at the laser source line frequency ν; $+/-T$ are the limits of integration. p can be related to the initial (I_ν^0) and transmitted (I_ν^t) laser beam intensities as shown.
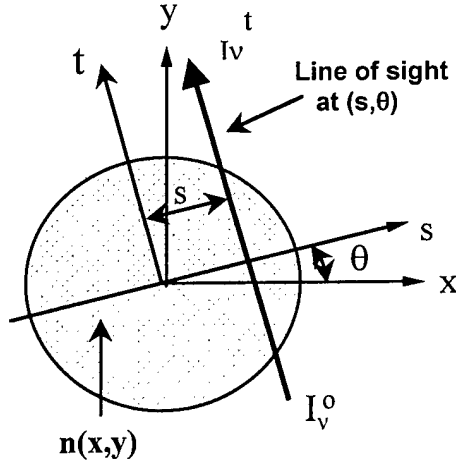

Figure 1. Schematic diagram of LOSs in single view and of coordinate system.

The practical reconstruction problem is to solve Eq. (1) for $n(x,y)$ in cases where $p(s,\theta)$ is known at a discrete set of s and θ. Because this reconstruction problem is ill-posed the solution or reconstruction method must be tuned to the problem at hand as defined by the character of $n(x,y)$ and the number and distribution over s and θ of the available projections $p(s_i, \theta_j)$.

In the case of chemiluminescence emission tomography, $p(s,\theta)$ is the line integral of the emission coefficient of the chemiluminescence, $j(x,y)$, integrated along the LOS defined by s and θ. As noted, the goal of these measurements is to reconstruct the distribution of the mean emission coefficient and components of its power spectral density function. In this case, $<j(x,y)>$ and components of it Fourier transform are reconstructed.

We have developed two reconstruction methods, both of which are series expansion methods. In the case of AFDDI, we expand n in a set of basis functions, b_k, with arguments $x-x_k$ and $y-y_k$, where x_k, y_k define the points of a triangular grid; $n = \Sigma f_k b_k$. In the original FDDI [1], there were 97 basis functions, and hence 97 unknown weighting factors to be found by solution of (1). For AFDDI, additional basis functions are added to the expansion at grid points located in regions of

4

high gradients in the original FDDI solution [2, 3]. In the second reconstruction method [4, 5] the basis functions are Karhunen-Loeve eigenfunctions of the training set, and in many cases relatively few functions are needed for a good representation of the distributions to be reconstructed.

IR Absorption and Flow Facilities

The IR absorption facility constructed for making LOS measurements on confined and unconfined, reacting and nonreacting flows is shown schematically in Fig. 2a. The facility consists of a Nd:YVO4-pumped, broadly tunable, KCl:Li color center laser (CCL) system and an optical apparatus composed of six scanning modules that permit simultaneous measurement of LOS absorption in a single plane at six different viewing angles, θ_j.

The CCL beam is electro-optically modulated for phase sensitive detection at a frequency of approximately 1 MHz. Each detector is connected to a demodulating "lock-in" circuit which beats the 1 MHz transmitted beam with a coherent reference signal at 1 MHz to generate a signal that represents the transmitted laser intensity as a function of time. The demodulated detector output is low-pass filtered at 50 kHz, read and processed by a fast PC-based data acquisition system. For each scanning module, the time history of the sweep signal is used to determine the transmission of the beam along selected LOSs. It takes approximately 1.5 milliseconds to complete a sweep.
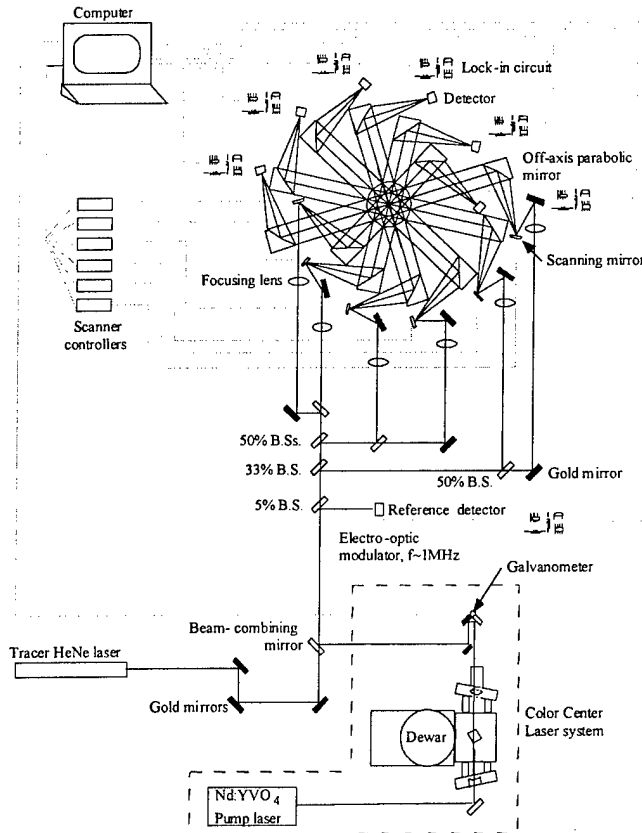

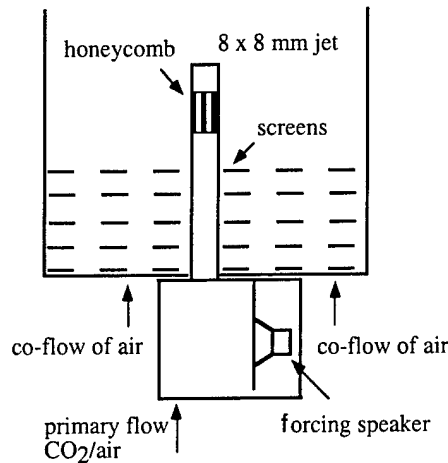**Figure 2a.** Schematic diagram of absorption apparatus.

Figure 2b. Schematic diagram of square jet flow apparatus.

Measurements have been made on a forced, square jet (8 mm x 8 mm) with a flow of a mixture of air and CO_2. The flow apparatus is shown schematically in Figure 2b. Gas flows are supplied from high pressure tanks and controlled by electronic mass flow controllers; total flow velocities up to 50 m/s are possible. Jet forcing at 30 Hz is provided by a speaker that is driven by an audio power amplifier. A stainless steel honeycomb is located near the exit of the jet in an effort to provide a uniform exit velocity profile. A chimney, exhaust hood, and co-flow of air are added to reduce the effects of ambient flow perturbations on the jet. Hot-wire anemometry is used to characterize the flow at the jet exit.

Proper Orthogonal Decomposition

In developing TRKB we have gained experience with POD analyses of sets of distributions. This experience has been applied to a POD analysis of the simulation results of Grinstein [9].

Detection and control of the large-scale features in combustion systems are of primary importance for mixing control in particular and combustion control in general. Reduced order models for representing the dynamics of a combustion system and large-scale structures are crucial to the development of combustion control. Proper Orthogonal Decomposition (POD), is one method used to develop reduced order models and investigate large-scale structures in combusting flows.

In POD, the Karhunen-Loeve procedure decomposes a set of distributions or functions into an optimal, orthonormal set of eigenfunctions able to represent the distributions of interest [4,5,6]. These eigenfunctions can offer highly efficient representations of important variables and structures in combustion systems. Furthermore, the potential for a reduced order models utilizing these basis functions can be evaluated from the associated eigenvalue spectrum derived from decomposition.

We have used the snapshot method [7] to obtain eigenfunctions and eigenvalues from CO_2 concentration and vorticity magnitude distribution sets of unsteady, reacting flows. These sets are from numerical computations using (LES) of turbulent reacting, forced rectangular jets of varying aspect ratios (AR=1-3) that were performed at the NRL [6,8,9]. The simulated (initially laminar) propane-nitrogen jets are issued into a quiescent oxygen-nitrogen background with a Mach number of 0.3 and Reynolds number greater than 85,000 based on the circular equivalent jet diameter. The jet exit velocity is forced axially by superimposing a single-frequency sinusoidal perturbation to the jet velocity U_o, having an rms level of 2.5 % and Strouhal frequency $St=fDe/U_o=0.5$, where De is the circular-equivalent diameter. Multi-species

temperature-dependent diffusion and thermal conduction processes are calculated explicitly using central difference approximations and coupled to chemical kinetics and convection using time step-splitting techniques. A global (single-step irreversible) model for propane chemistry is used [10]. Further details on the simulated transport properties and their validation are discussed in [8], [9] and references therein.

Results of Measurements, Reconstruction Algorithm Refinement and POD Analysis

Forced Square Jet Measurements Measurements were made in both laminar and forced jets with velocities ranging from 1 to 50 m/s and varying CO_2 concentrations. Absorption data were obtained simultaneously in six different viewing angles in approximately 1.5 ms. The output from the lock-in amplifier circuit for each module was over sampled by the data acquisition system to help reduce the influence of electrical noise. Sample results are shown in figure 3 where it can be seen that the combination of phase sensitive detection and over sampling gives very low noise projection data.
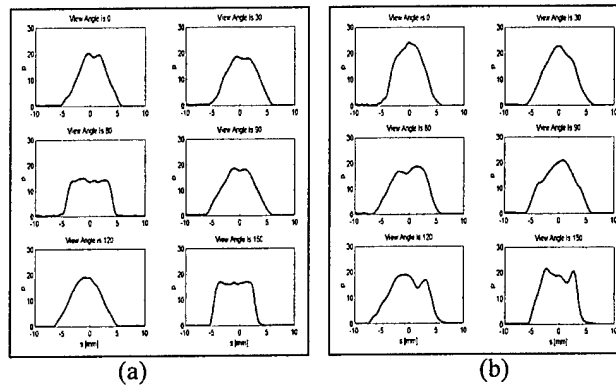

(a)   (b)

Figure 3. Two sets of measured projection data from a 6 m/s forced jet with 50% CO_2 made at the same phase in the forcing. (a) Measurements made near the jet exit. (b) Measurements made 1 *De* downstream of the jet exit.

The projection data shown in figure 3 were obtained from measurements made in a 6 m/s jet with 50% CO_2 at one *De* downstream of the jet exit. For each set of projection data, the location and shape of the CO_2 absorption profile is slightly different in each of the views because the jet is not centered in the domain and is not axisymmetric. Electrical noise and ambient CO_2 concentration fluctuations in regions outside of the measurement domain are the most significant sources of error in the projection measurements. Care was taken to reduce the concentration fluctuations as much as possible.

Forced Square Jet Reconstructions Inversion of the projection data from module measurements was performed using the AFDDI method as it has been shown to consistently lower reconstruction errors over those resulting from original FDDI; see below. 175 LOSs for each view angle (1050 total) were used to reconstruct concentration fields. AFDDI reconstructions often showed nonphysical features that were due in part to the reconstruction method (reconstruction artifacts) and associated primarily with limitations on the number of basis functions allowed. To reduce these features a Gaussian spatial filter with a full-width at half max equal to twice the smallest spacing of points on the adaptive triangular grid was applied to the reconstruction results. The filter does a good job of removing the artifacts while retaining the large-scale features of the concentration field. The filtered AFDDI reconstructions obtained from
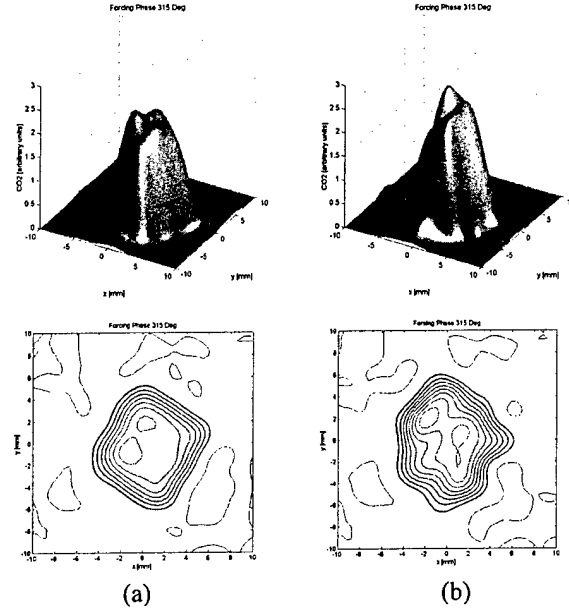
7

Figure 4. Filtered AFDDI reconstructions of a 6 m/s, 50% CO_2 forced jet and corresponding contour plots from data of Figure 6 showing forced jet CO_2 concentration distributions at a forcing phase angle of 315 deg. (a) Measurements near the jet exit. (b) Measurements 1 *De* downstream of the jet exit.

the projection data given in figure 3 are presented in figure 4. These results show little effect of forcing. Reconstructions of the CO_2 concentration field at the jet exit are approximately the same for the eight forcing phases studied. Results at 1 De downstream show slight spreading of the jet and slight changes in shape with changing phase angle but overall forcing appears to have very little influence. At lower jet velocities the influence of forcing is more evident.
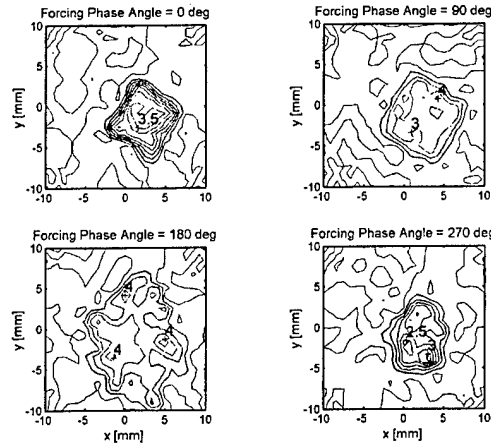

Figure 5. Contour plots of reconstructions at 4 different phase angles of a 3 m/s, 25 % CO_2 jet at approximately 1 *De* downstream of the jet exit. Measurements are made at 0, 90, 180 and 270 degrees in the forcing phase. Maximum CO_2 values are labeled on the plots in arbitrary units.
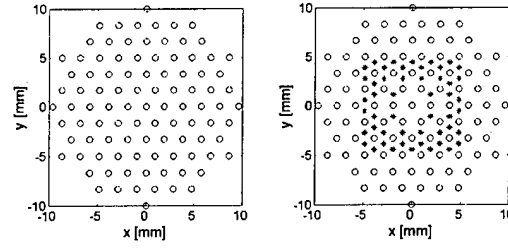
Figure 6. Adaptive grid for the phantom distribution presented in figure 7. Left: uniform grid of 97 basis functions. Right: Adaptive grid with the original 97 basis functions (o) and 50 additional basis functions (*) in regions of high gradient.

Figure 5 shows contour plots of four forced-jet reconstructions from data collected on a 3 m/s jet with 25% CO_2 at approximately 1 De downstream from the jet exit. Here data were taken at 90° phase increments relative to the jet forcing signal. Significant modulation of the jet flow is apparent in these reconstructions. The square structure of the jet is evident at phases of 0 and 90 degrees. The jet has begun to spread at the 90 degree phase and more significantly by 180 degrees. At the 270 degree phase, the extent of the jet has been diminished, approximating that of the jet at 0 degrees but with a lower peak CO_2 concentration. Compared to the 6 m/s jet, these results show significant changes due to the forcing.

Refinement of FDDI The majority of the jet flows we have studied have square, top-hat like
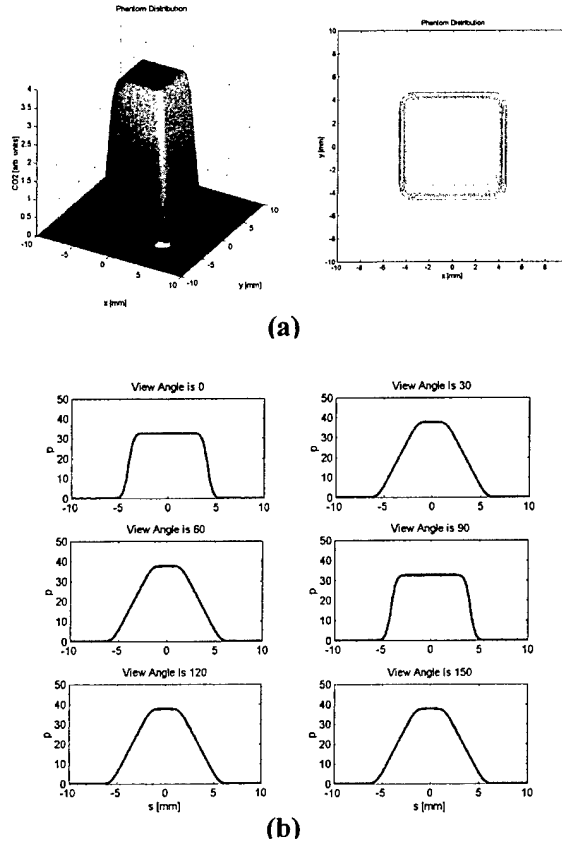

(a)

(b)

Figure 7. Square top-hat phantom distribution and corresponding phantom projection data.

9

concentration profiles with steep, smooth sides and relatively flat tops. These features are difficult to reconstruct accurately and represent a significant challenge for tomographic reconstruction methods. We investigated strategies for improving the AFDDI method to better reconstruct these features. In the original FDDI, 97 identical basis functions located on a uniform triangular grid were used for tomographic reconstruction [1]. In AFDDI, 97 basis functions were used on the original grid and 50 basis functions were added in regions of high concentration gradients. Sample grids are presented in figure 6 for the phantom test distribution shown in
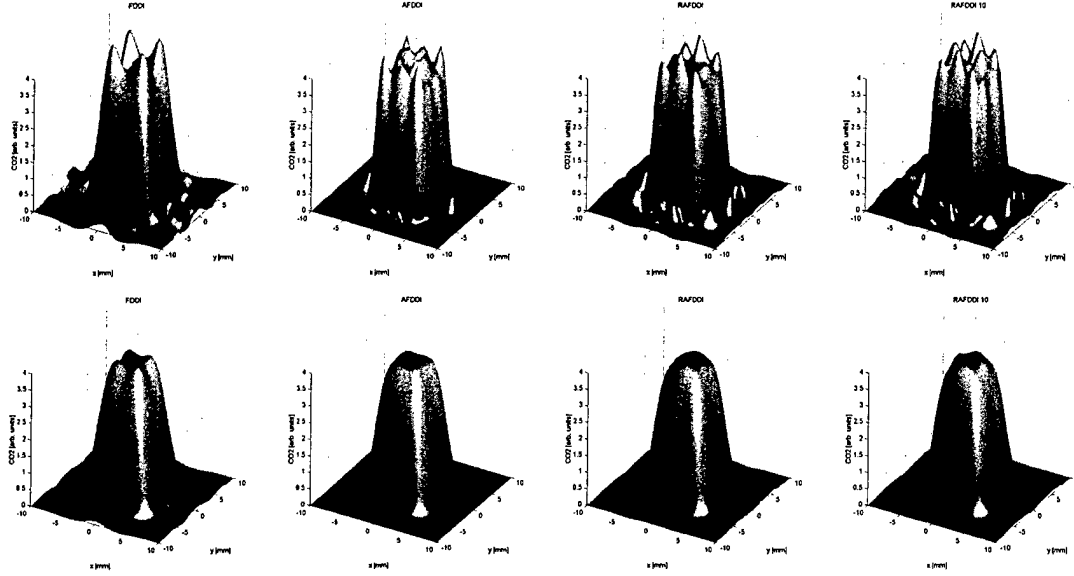

Figure 8. Reconstructions of phantom distribution shown in figure 7. Top row: Unfiltered reconstructions. Bottom row: Filtered reconstructions. From left to right: FDDI, AFDDI, RAFDDI, and RAFDDI 10 reconstructions.

figure 7. All 147 of the basis functions initially used in AFDDI were identical and had a higher aspect ratio than that of the original FDDI basis functions.

One refinement of AFDDI considered was the use of different aspect ratio basis functions. In Refined Adaptive FDDI (RAFDDI), the high aspect ratio basis functions from AFDDI were used at the locations of the additional 50 basis functions and low aspect ratio basis functions (from FDDI) were used on the original 97 grid points. In RAFDDI 10 the aspect ratios of the 10 basis functions on the original grid that lie in the highest gradient regions are the same as those located on the 50 added grid points. Numerically generated phantom distributions and corresponding projection data were used to test these changes in the reconstruction method.

The phantom distribution and corresponding projection data used for testing are those of a smoothed square, top-hat jet as shown in figure 7. The results of reconstructions of this distribution are shown in figure 8. It can be seen in the plots that AFDDI does a good job of capturing the steep gradients of the phantom distribution while reducing the artifacts seen on the top of the peak. This structure is still evident but is not as severe as in the FDDI reconstruction. When smoothed with the Gaussian filter discussed in the previous section, the AFDDI reconstruction does a better job of approximately the flatness of the original phantom distribution than any of the other methods used. The AFDDI reconstruction also reduces significantly the reconstruction artifacts around the base of the jet relative to the other methods.

Three error measures are often used for quantitative comparisons: 1) the normalized root mean square error, e_{rms}; 2) the normalized mean absolute error, e_{abs}; and 3) the maximum error, e_{max}. e_{rms} emphasizes a few large errors in the reconstruction, while e_{abs} emphasizes many small errors. The error measures are defined as

$$e_{rms} = \frac{\left\| n_1 - n_0 \right\|_F}{\left\| n_0 - \overline{n_0} \right\|_F}$$

$$e_{abs} = \frac{\overline{\left| n_1 - n_0 \right|}}{\overline{\left| n_0 \right|}} \qquad (4)$$

$$e_{max} = \frac{\max\left(\left| n_0 - n_1 \right| \right)}{n_0 \left(x_{max}, y_{max} \right)}$$

where n_0 is the reference distribution, in this case, the phantom distribution, and n_1 is the reconstructed distribution to be evaluated. $\| \ \|_F$ denotes a Frobenius norm and the overbar denotes a spatial average.

Error measures for the reconstructions in figure 8 are presented in tables 1 and 2, where it is seen that the AFDDI reconstruction shows the lowest root mean square and absolute errors. Reconstructions using RAFDDI and RAFDDI 10 show higher e_{rms} and e_{abs} than errors resulting from AFDDI but remain lower than the errors resulting from the original FDDI method. Comparisons of the filtered reconstruction errors also show that AFDDI produced the smallest errors for the three error measures. Visual inspection of the filtered reconstructions in figure 8 shows only small differences between these reconstructions. Also it is noted that smoothing of the highest gradient regions due to filtering has caused the reconstruction errors to increase over those of the unfiltered reconstructions.

Table 1: Error measures for unfiltered reconstructions of the phantom distribution in Figure 10.

Table 2: Error measures for filtered reconstructions of the phantom distribution in Figure 10.

POD results. Proper orthogonal decomposition has been used to analyze ensembles of concentration and vorticity magnitude distributions in forced reacting rectangular jets of aspect ratios 1-3 [6]. Ensembles were constructed at various downstream locations using CO_2 concentration and vorticity data from LES [8, 9] and contained 60 and 63 ensemble members, respectively. Through evaluation of the eigenvalue spectra (see figure 10), it was determined that there is a stronger potential for reduced-order modeling based on the CO_2 field than based on the vorticity field, while this potential is approximately the same for the different rectangular jets studied - aspect ratios 1, 2, and 3. Physical insight was gained through examination of the K-L eigenfunctions, specifically relating to vortex structures and the development of the CO_2 concentration field through mixing and spreading at locations downstream from the jet exit [6]. Axis-switching phenomena and the influence of vortex dynamics on mixing were also evident in the POD eigenfunctions [6].

Sample POD eigenfunctions are presented in Figure 11. Note that the CO_2 and vorticity eigenfunctions for each jet are closely related in shape and spatial extent, indicating the strong influence of vorticity on mixing.
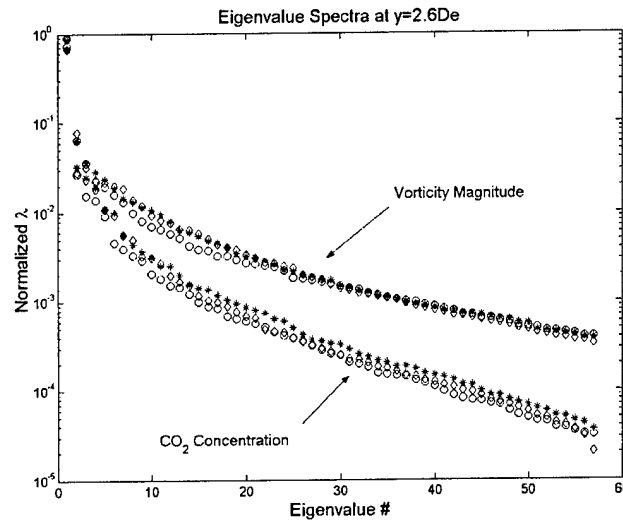

Figure 10. Eigenvalue spectra of CO_2 and vorticity magnitude results at y=2.6De. The faster decrease with eigenvalue number of CO_2 eigenvalues than vorticity eigenvalues indicates a better potential for reduced order modeling of the CO_2 field than for vorticity.
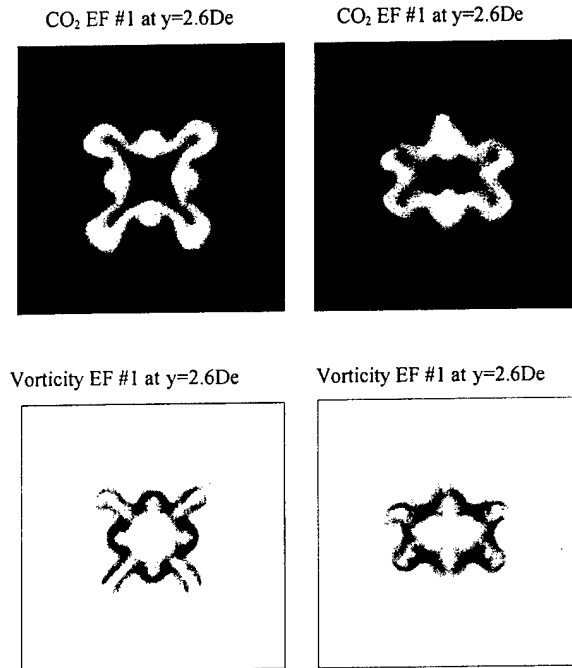
12

CO₂ EF #1 at y=2.6De   CO₂ EF #1 at y=2.6De

Vorticity EF #1 at y=2.6De   Vorticity EF #1 at y=2.6De

Figure 11. First eigenfunctions of CO_2 concentration (top) and vorticity magnitude (bottom) for $AR=1$ (left) and $AR=2$ (right) jets.

Chemiluminescence Camera

Work on the development of a linear array equipped 35 mm camera system was begun during the last year of the grant. The system would be used for chemiluminescent emission tomography studies of heat release dynamics. The intensity of chemiluminescent emissions is known to be closely coupled to combustion heat release rates, and for this reason chemiluminescent emission measurements are widely performed. Chemiluminescence emission tomography can be used to measure the spatially resolved mean of these emissions and spatially resolved features of their power spectral densities; these features are signatures of local heat release fluctuation dynamics. To perform these measurements a 32 element, array detector is mounted in the focal plane of a 35 mm single lens reflex (SLR) camera. After amplification and filtering the output of each array element is stored on a PC for data analysis. This analysis includes FFT and spectral analyses of the array element signals and reconstruction of interesting frequency components of the power spectra and the spatial distribution of the mean emissions. By mounting the detectors in a 35 mm camera we will have a measurement system that is compact, highly portable and easy to use.

In collaboration with Dr. Robert Schefer of Sandia National Laboratories we have designed and built a prototype camera and amplifier circuit. Preliminary measurements on a swirl flow, gas fired laboratory combustor have demonstrated the potential of the camera system, and work is proceeding to refine the detector electronics and to develop signal analysis and tomographic reconstruction software. Further testing and collaboration with Sandia are planned.

Summary

Significant progress on the development of tomography for sensing and the application of tomography to the study of forced jets have been made over the course of the grant. In

addition the structure of forced rectangular reacting jets and the potential for reduced order modeling of such jets have been investigated by the POD analyses jet simulations. The AFDDI reconstruction method has been refined by including basis function optimization and filtering and has been used to determine 2D concentration distributions from the 1D projection data acquired by our absorption tomography facility. This facility was developed with ONR support and through phase sensitive detection and over sampling provides low noise absorption data for tomography. The refinement of AFDDI has lead to better reconstructions of the top hat concentration profiles characteristic of square and rectangular jets. POD analyses have been completed on computational combustion simulations of forced, rectangular jets with aspect ratios of 1, 2, and 3 performed at the NRL. Results of the analyses indicate that the CO_2 concentration profiles, and to a lesser extent the vorticity profiles, can be well represented by a reduced order model. This result shows promise for the development of a combustion control system. Finally, the development of linear array cameras and software for chemiluminescence emission tomography measurements has been initiated and in collaboration with Dr. Schefer of Sandia the feasibility of such a camera has been demonstrated.

Our work on tomography will continue in two directions. One is the chemiluminescence tomography work just cited. The other is work with P&W to help them develop an IR absorption sensor for the temperature pattern factor at the exit of a research combustor. The sensor will use a diode laser based measurement system following work at Stanford. Our task will be to advise on the measurement configuration and help with data analysis.

References

1. Ravichandran, M. and Gouldin, F.C. "Reconstruction of smooth distributions from a limited number of projections," *Applied Optics*, 27:4084, 1988.

2. Ha, J., Feng, M. and Gouldin, F.C. "Laser tomographic reconstruction in a complex concentration flow field," *AIAA-99-0444*, 1999.

3. Feng, M. and Gouldin, F. C. "Experimental Evaluation of An Adaptive Tomographic Inversion Method," *AIAA 2000-0949*, 2000.

4. Torniainen, E. D., Ph.D. thesis, Cornell University, Ithaca, NY, 2000.

5. Torniainen, E. D., Hinz, A., and Gouldin, F. C. "Tomographic Analysis of Unsteady, Reacting Flows," *AIAA J*, 36: 1270-1278, 1998.

6. Edwards, J., Gouldin, F., Grinstein, F., and Kailasanath, K. "Reduced Order Structure of Reacting Rectangular Jets, *AIAA 2002-1011*, 2002.

7. Sirovich, L. and Everson, R. "Management and analysis of large scientific data sets," *Int. J. of Supercomputer Applications*, 6:50, 1992.

8. Grinstein, F.F. and Kailasanath, K., "Exothermicity and Three-Dimensional Effects in Unsteady Propane Square Jets", in *26th International Symposium on Combustion*, The Combustion Institute, Pittsburgh, pp. 91-96 (1996).

9. Grinstein, F.F., Vortex Dynamics and Entrainment in Rectangular Free Jets, *Journal of Fluid Mechanics*, 437: 69-101 (2001).

10. Westbrook, C.K. and Dryer, F.L., "Chemical Kinetic Modeling of Hydrocarbon Combustion", *Combust. Sci. and Tech.*, **27**: 31-43, (1981).

11. Feng, M., Gouldin, F. and Edwards, J., "Scanning for High Speed Laser Absorption Tomography", AIAA 2001-09711, January 2001.

12. Edwards, J., Gouldin, F. and Macdonald, M., "High Speed Absorption Tomography With Advanced Reconstruction Algorithms", AIAA-2003-1013, 2003.

Appendix 1. Personnel working on the Grant

F. C. Gouldin, PI

G. J. Wolga, co-PI

Ann Chojnecki, post doctoral associate

Mark McDonald, post doctoral associate

Jennifer Edwards, PhD student

Michel Feng, PhD student

Colin Smith, undergraduate student

Ryan Beresky, undergraduate student

Appendix 2. PhD Theses wholly or partially support on Grant

Michel Feng, "Development of a Real Time Tomography System for Combustion", August 2000.

Jennifer Edwards, Tomography and POD Applied for Combustion Control, May 2004 (tentative).

Appendix 3. Papers and Publications

Papers:

M. Y. Feng and F. C. Gouldin, Experimental Evaluation of An Adaptive Tomographic Inversion Method, AIAA-2000-0949, January 2000.

M. Feng, F. C. Gouldin and J. L. Edwards, Scanning For High Speed Laser Absorption Tomography, AIAA-2001-0791, January 2001.

Jennifer L. Edwards, Frederick C. Gouldin, Fernando F. Grinstein, and Kazhikathra Kailasanath, Reduced Order Structure of Reacting Rectangular Jets, AIAA-2002-1011, January 2002.

Jennifer L. Edwards, Frederick C. Gouldin, Mark A. MacDonald, High Speed Absorption Tomography With Advanced Reconstruction Algorithms, AIAA-2003-1013, January 20003.

Publications in preparation:

Jennifer L. Edwards, Frederick C. Gouldin, Fernando F. Grinstein, and Kazhikathra Kailasanath, Reduced Order Structure of Reacting Rectangular Jets, in preparation for AIAA J.

Jennifer L. Edwards, Frederick C. Gouldin, Mark A. MacDonald, High Speed Absorption Tomography With Advanced Reconstruction Algorithms, in preparation.

Book chapter:

F. C. Gouldin and J. L. Edwards, "Infrared Absorption Tomography for Active Combustion Control", Chapter 16 in **Control of Combustion Processes,** G. Roy, edt., 2003.

REPORT DOCUMENTATION PAGE

Form Approved
OMB No. 0704-0188

1. REPORT DATE *(DD-MM-YYYY)*	2. REPORT DATE	3. DATES COVERED *(From - To)*
31/07/03	Final Technical Report	01/05/99 – 31/04/03

4. TITLE AND SUBTITLE	5a. CONTRACT NUMBER
IR Absorption Tomography for Active Combustion Control	5b. GRANT NUMBER N00014-99-0447
	5c. PROGRAM ELEMENT NUMBER

6. AUTHOR(S)	5d. PROJECT NUMBER
F.C. Gouldin	5e. TASK NUMBER
	5f. WORK UNIT NUMBER

7. PERFORMING ORGANIZATION NAME(S) AND ADDRESS(ES)	8. PERFORMING ORGANIZATION REPORT NUMBER
Cornell University Office of Sponsored Programs 115 Day Hall, Ithaca, NY 14850	

9. SPONSORING/MONITORING AGENCY NAME(S) AND ADDRESS(ES)	10. SPONSOR/MONITOR'S ACRONYM(S)
Dr. Gabriel Roy, ONR333 Office of Naval Research, Ballston Ctr. Tower One 800 N. Quincy Street Arlington, VA 22217-5660	ONR
	11. SPONSORING/MONITORING AGENCY REPORT NUMBER

12. DISTRIBUTION AVAILABILITY STATEMENT
APPROVED FOR PUBLIC RELEASE

13. SUPPLEMENTARY NOTES

14. ABSTRACT: The research goals were 1) to further the development of IR absorption tomography as a sensor for active control of combustion systems, 2) to apply IR absorption tomography to study mixing in forced-jet actuators, 3) to use POD analysis to study large scale structures in reacting jet flows and the potential for reduced order models of these flows and 4) to develop a camera system for chemiluminescence studies of combustion heat release dynamics. The research was in collaboration with Drs. Grinstein and Kailasanth of the NRL and with Dr. Schefer of Sandia National Laboratories. Major accomplishments were 1) completion of an IR absorption facility and measurements on forced, square jets, 2) refinement of the tomographic reconstruction algorithm Adaptive Finite Domain Direct Inversion, 3) analysis of large eddy simulations of forced, reacting rectangular jets using POD that showed a good potential for reduced order modeling, and 4) development of a linear array equipped 35mm camera and data analysis software for chemiluminescence emission tomography. Work on this Grant was a significant portion of two Ph. D. theses, was reported in four AIAA preprints and is the subject of two papers in preparation for publication and an article appearing in a book based on papers presented at the 15th ONR Propulsion Meeting.

15. SUBJECT TERMS

Active Combustion Control, Absorption Tomography, Proper Orthogonal Decomposition

16. SECURITY CLASSIFICATION OF:			17. LIMITATION OF ABSTRACT	18. NUMBER OF PAGES	19a. NAME OF RESPONSIBLE PERSON
a. REPORT	b. ABSTRACT	c. THIS PAGE			Jeff Corbin
U	U	U	UU	16	19b. TELEPONE NUMBER *(Include area code)* 607-255-6306

Standard Form 298 (Rev. 8-98)
Prescribed by ANSI-Std Z39-18